

**USE OF SILHOUETTE EDGES AND AMBIENT  
OCCLUSION IN PARTICLE VISUALIZATION**

by

James L. Bigler

A thesis submitted to the faculty of  
The University of Utah  
in partial fulfillment of the requirements for the degree of

Masters of Science

in

Computer Science

School of Computing

The University of Utah

August 2004

Copyright © James L. Bigler 2004

All Rights Reserved

THE UNIVERSITY OF UTAH GRADUATE SCHOOL

## SUPERVISORY COMMITTEE APPROVAL

of a thesis submitted by

James L. Bigler

This thesis has been read by each member of the following supervisory committee and by majority vote has been found to be satisfactory.

---

---

Chair: Charles D. Hansen

---

---

Steven G. Parker

---

---

Peter Shirley

THE UNIVERSITY OF UTAH GRADUATE SCHOOL

**FINAL READING APPROVAL**

To the Graduate Council of the University of Utah:

I have read the thesis of James L. Bigler in its final form and have found that (1) its format, citations, and bibliographic style are consistent and acceptable; (2) its illustrative materials including figures, tables, and charts are in place; and (3) the final manuscript is satisfactory to the Supervisory Committee and is ready for submission to The Graduate School.

\_\_\_\_\_  
Date

\_\_\_\_\_  
Charles D. Hansen  
Chair: Supervisory Committee

Approved for the Major Department

\_\_\_\_\_  
Chris R. Johnson  
Chair/Director

Approved for the Graduate Council

\_\_\_\_\_  
David S. Chapman  
Dean of The Graduate School

## **ABSTRACT**

Particle visualization has traditionally borrowed techniques from grid based methods. Some grid based methods such as shadows and the Phong illumination model are easily applied to the particle renderings which often use iconic shapes such as spheres and ellipsoids to represent the data. While these approaches are appropriate for particle based data, not all grid based visualization methods are suitable for particle visualization. This thesis investigates the use of image based silhouette edges and ambient occlusion textures with respect to particle visualization demonstrating the effectiveness of these techniques.

To my wife, Laura

# CONTENTS

<b>ABSTRACT</b> .....	<b>iv</b>
<b>LIST OF FIGURES</b> .....	<b>vii</b>
<b>LIST OF TABLES</b> .....	<b>x</b>
<b>ACKNOWLEDGMENTS</b> .....	<b>xi</b>
<b>CHAPTERS</b>	
<b>1. INTRODUCTION</b> .....	<b>1</b>
<b>2. BACKGROUND</b> .....	<b>6</b>
<b>3. AMBIENT OCCLUSION</b> .....	<b>10</b>
3.1 Data precomputation and storage .....	10
3.1.1 Texture Mapping .....	10
3.1.2 Ambient value computation .....	11
3.1.3 Texture dilation .....	13
3.1.4 Final post processing .....	15
3.2 Render phase .....	15
3.3 Analysis .....	16
3.3.1 Precomputation Time .....	16
3.3.2 Impact on rendering time and memory .....	17
3.3.3 Perceptual results .....	19
<b>4. SILHOUETTES</b> .....	<b>26</b>
4.1 Depth buffer from ray tracing .....	26
4.2 Generating silhouette edges from the depth buffer .....	27
4.3 Analysis .....	29
<b>5. CONCLUSIONS AND FUTURE WORK</b> .....	<b>35</b>
5.1 Ambient Occlusion .....	35
5.2 Silhouette edges .....	38
5.3 Final comments .....	39
<b>REFERENCES</b> .....	<b>41</b>

## LIST OF FIGURES

1.1	Tensor values can be used to deform and rotate spheres representing particles into ellipsoids . . . . .	3
1.2	Local lighting models can help show particle boundaries. The left image had no lighting, the right includes phong shading. . . . .	4
1.3	Aliasing can have a negative effect on the visualization process. . . . .	4
1.4	Without shadows, it is difficult to determine how far the red block is from the surface (left). Shadows can disambiguate this (center, left). . . . .	5
2.1	An isosurface representing a human skull with a fracture of bones in the right hand jaw. Vicinity shading helps the perception of space between the jaw bones and the rest of the skull. The image on the left has only phong illumination. The image on the right shows the vicinity values. The center image is the combination of the left and right images. <i>Image used by author's permission</i> . . . . .	8
3.1	To texture a sphere using two a two dimensional mapping, one dimension corresponds to latitude the other to longitude. . . . .	11
3.2	Jittered sampling divides the domain into regions and assigns a single point a random location for each cell. . . . .	12
3.3	Bilinear interpolation can cause artifacts in regions where particles overlap. The dark banding that can be seen between the particles are caused by interpolating values that exists inside other particles with values that are outside. . . . .	13
3.4	By dilating values that are outside to ones inside, interpolation errors can be reduced without introducing new errors. . . . .	14
3.5	Determining if a ray is inside or outside by means of the dot product of the normal and ray direction works for ray $a$ , but not for ray $b$ . . . . .	15
3.6	By wrapping the textures across the U parameter the seam can be eliminated. . . . .	16
3.7	Ambient occlusion shading texture values mapped on the Fireball 11 data set. The views are identical to the ones in Figure 3.8. Sub-images are referred to as A, B, and C, left to right. . . . .	21
3.8	Ambient occlusion shading texture values mapped on the Fireball 11 data set. The views are identical to the ones in Figure 3.7. Sub-images are referred to as A, B, and C, left to right. . . . .	21

3.9	Ambient occlusion shading texture values mapped on the Cylinder 06 data set. Notice how the intricate structure is quite visible on the center of the structure. The spheres that protrude further from the front surface are clearly seen to do so. The views are identical to the ones in Figure 3.10. Sub-images are referred to as A (left) and B (right).	22
3.10	Ambient occlusion shading texture values mapped on the Cylinder 06 data set. One thing to note is the ability to see the two spheres standing out in front of the hole. The views are identical to the ones in Figure 3.9. Sub-images are referred to as A (left) and B (right).	22
3.11	Ambient occlusion shading texture values mapped on the Bullet 02 data set. Sub-images are referred to as A, B, and C, left to right. Figure A is provides a view of the whole data set, while B and C show some close ups. The relative positions of the bullet with the material are easily perceived. The views are identical to the ones in Figure 3.12.	23
3.12	Ambient occlusion shading texture values mapped on the Bullet 02 data set. Sub-images are referred to as A, B, and C, left to right. Figure A is provides a view of the whole data set, while B and C show some close ups. As with Figure 3.11, the relative positions of the bullet with the material as well as inside the holes in the objects are easily perceived. The views are identical to the ones in Figure 3.11.	23
3.13	The image on the left is without ambient occlusion information. The one on the right includes the ambient shading.	24
3.14	As the data is cropped, the ambient occlusion shading values are no longer applicable. The far left images show the uncropped data set. The center and right images show progressive cropping of the data. The internal particles that were not visible before the cropping are erroneously dark.	24
3.15	The images above show the visualization with the ambient occlusion values combined with direct lighting. The lower images use only the direct lighting contribution. The image on the left is the uncropped data. Images in the center and right hand sides show two different croppings.	25
4.1	The depth buffer and the corresponding image generated using RTRT. The values for the depth buffer have been quantize in such a way as to make the foreground discontinuities more visible.	27
4.2	Second derivative kernels are very sensitive to noise, and usually require smoothing the input first to produce reasonable results. The image on the left is the original image. The center image is made by thresholding the Laplacian without any smoothing. The right side image smoothes the image using a Gaussian, convolves with the Laplacian, and thresholds the values.	28
4.3	Laplacian Kernel	28

4.4	The left most column contain images where the edges are assigned by using the absolute value of the Laplacian compared with a threshold. The second column from the left is where only the positive values of the Laplacian are greater than a threshold. The right two columns of images show the edges applied to the rendered image. The top row of images compare the Laplacian to a threshold of 0, while the lower images use progressively smaller and smaller thresholds encompassing more and more edges. . . . .	31
4.5	Silhouettes over each particle can be useful showing trends in particle placement, especially without shadows . . . . .	32
4.6	The same data and view as Figure 4.5, but with shadows . . . . .	32
4.7	By varying the threshold of the Laplacian to be counted as an edge we can change how many edges are displayed. The upper left image shows no silhouettes. The upper right and lower left show progressively more and more edges. The lower right image, shows all the detectable edges. . . . .	33
4.8	These images show the use of silhouette edges with and without shadows. The images are referred to as A (top left), B (top right), C (bottom left), and D (bottom right). Images on the top have shadows, while images on the left have silhouette edges. . . . .	34
5.1	This data depicts a foam structure being crushed. The top images are with direct lighting only with color mapping. The bottom images show the ambient occlusion values applied to the data set. Images on the right contain silhouette edges, the ones on the left do not. . . . .	37

## LIST OF TABLES

3.1	Approximate time to generate textures for varying data sets. All times given are for 49 samples per texel with 16x16 (256) texels per sphere (12544 samples per sphere). Computation was done using 20 processors on an SGI Origin 3800 with 600 MHz R14K processors. Images using the textures are also referenced. . . . .	17
3.2	Extra memory required to store the ambient value textures for various data sets. . . . .	18
3.3	Relative frame rates for a series of views and data sets. Computation was done using 20 processors on an SGI Origin 3800 with 600 MHz R14K processors. The image rendered was 500x500 pixels except Bullet 2 and Bullet 12 which were 250x500 to match the images. . . .	18
4.1	Relative frame rates for a series of views and data sets. Computation was done using 20 processors on an SGI Origin 3800 with 600 MHz R14K processors. The resolution of the images rendered is 500x500 pixels. . . . .	29

## ACKNOWLEDGMENTS

I would like to thank the following individuals and organizations.

- My family, especially Laura for all the love and support
- My advisor, for helping to provide the vision and direction that helped me get through this.
- Steve, for being such a great boss and mentor.
- Pete, he's the man!
- Christiaan Gribble, for a friendly ear and jointly writing much of the code used for the vicinity shading computation.
- C-SAFE and DOE, for the funds to do this research.
- SCI, for providing an atmosphere that makes collaboration happen.
- Jim Guilkey, for data, feedback, and plenty of sas.

# CHAPTER 1

## INTRODUCTION

Computational simulation is a way to explore and understand the world around us. In order to do so, often the interaction of materials with their surroundings must be computed. This calculation is frequently done on grids, however grids are not well suited for complicated geometry where the grid would have to be refined beyond computational capabilities. Implicit surfaces could be used to deal with the resolution problem, unfortunately the complexity of the equations defining intricate surfaces make their use prohibitive. Instead, structures made up of discrete pieces of material can be represented using particles.

Particle methods for computation have been used to simulate many different phenomenon in scales ranging from the evolution of the universe to the iteration of atoms on a molecular scale. In astronomical simulations particles can represent large bodies of mass and are often used to compute N-body problems where forces such as gravity can be computed for each piece of matter. Atomic simulations represent individual atoms as particles that interact with the other atoms using such forces as atomic potential and attraction. Simulations in this scale seek to know how individual molecules are formed or how they react with other molecules. As the scale increases the amount of matter represented by particles can change to accommodate the limits of computation.

One particular application of particles in simulation is the Material Point Method (MPM)[4]. Objects and material in the simulation are represented with particles. This allows for arbitrary shape and changes in this shape as the simulation progresses. At the beginning of each time step values from the particles are interpolated to a grid. This grid is usually of a coarser resolution than the particles meaning there

are more particles in relation to node points. CFD computation is then performed on the grid and values are re-interpolated to the particles and their locations are updated. MPM has advantages over strictly grid based methods in that contact between material does not have to be explicitly computed as in a finite element approach.

One way to view the results of particle simulations is to interpolate values onto a regular grid and visualize the data using traditional grid based methods such as isosurfacing and direct volume rendering. However this has several disadvantages. Areas where the particles are sparse can result in incorrect structure reconstruction missing features too fine for the chosen grid resolution. To compensate for this, grids must be refined beyond the resolution of the particles. Also, memory is wasted representing areas that do not need refinement, such as regions without data or where the values are varying smoothly. Representing particle data as a regular grid can also mask the fine structure which may exist in the original form. Certain types of particle data, such as molecular simulations, do not have an analog in grid based representations and thus pose a problem in using this representation.

It is clear there exists a need to view particle data in a way that is both appropriate and informative. What does this mean? Since particle data seeks to represent pieces of a larger whole, the ability to see and interpret the macroscopic structure created by these particles is vital. As well, the ability to view fine structure is important for particle visualization. Appropriate visualizations are those which add to the overall understanding of the data while minimizing erroneous interpretations of it. There are two main goals of particle visualization. The first is the structure which is represented by the actual placement and sizes of the particles. The second are qualitative trends in values associated with the particles such as mass, speed, or stress.

Particle visualization often takes the form of rendering the data as spheres to represent the location and size of the particles used in simulation. Color mapping scalar quantities associated with particles (such as mass, volume, and speed) is an additional method used to obtain a qualitative understanding of the data. Other

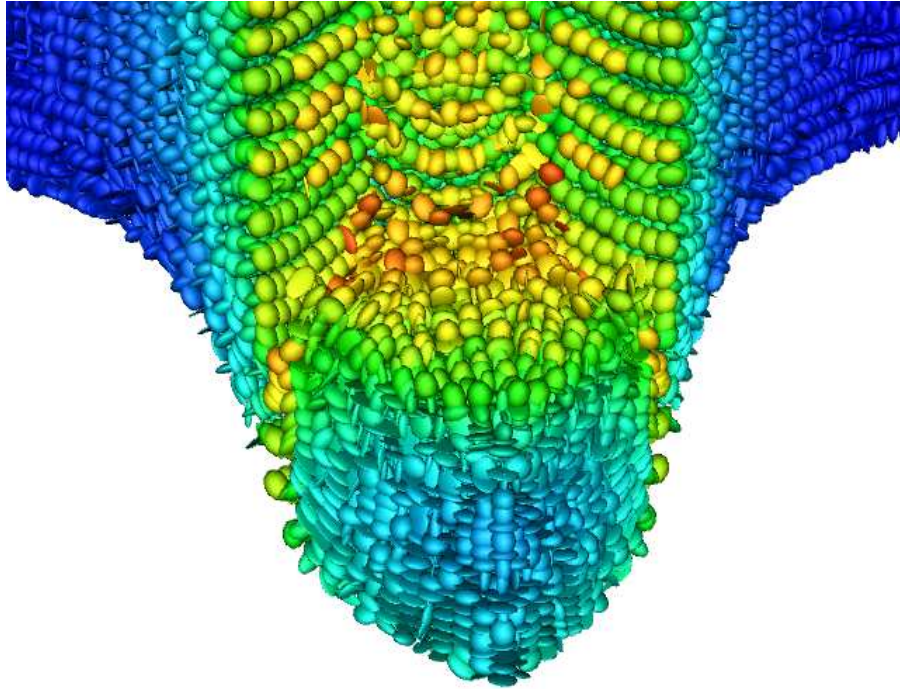


**Figure 1.1.** Tensor values can be used to deform and rotate spheres representing particles into ellipsoids

methods of applying particle values to the dataset include particle deformation and rotation resulting in ellipsoid or super-ellipsoid primitives (Figure 1.1).

Lighting models can be used to provide spatial information. Renderings which make no use of lighting make it difficult to distinguish one particle from another (Figure 1.2). The use of a local lighting model such as Phong generated specular highlights can aide in seeing boundaries of particles and the three dimensional structure of individual particles, but can introduce other problems. One such problem is aliasing[1]. As the particles become near to or smaller than a pixel, features from the lighting model create high frequency changes in the images resulting in aliasing. This is distracting to the perception of the overall structure of the data as seen in Figure 1.3.

Local lighting models also fail to aid in the perception of the spatial relationships of particles with each other. This global information cannot be accurately captured with a local model. As seen in Figure 1.4 using a global operation, such as shadows,

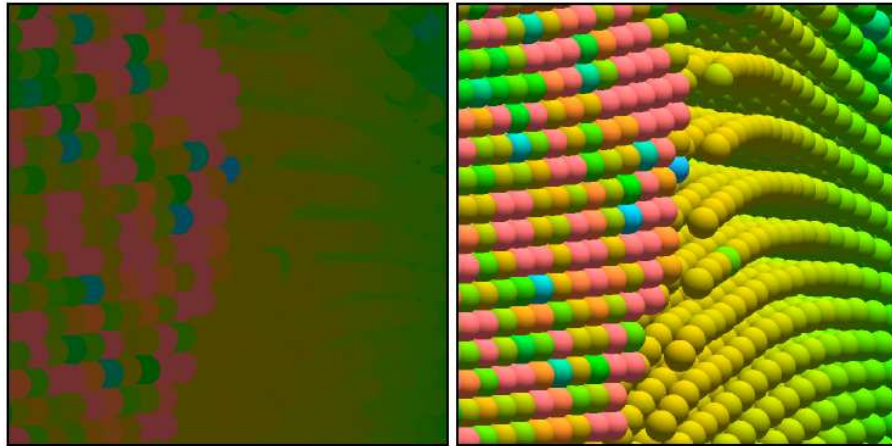


**Figure 1.2.** Local lighting models can help show particle boundaries. The left image had no lighting, the right includes phong shading.

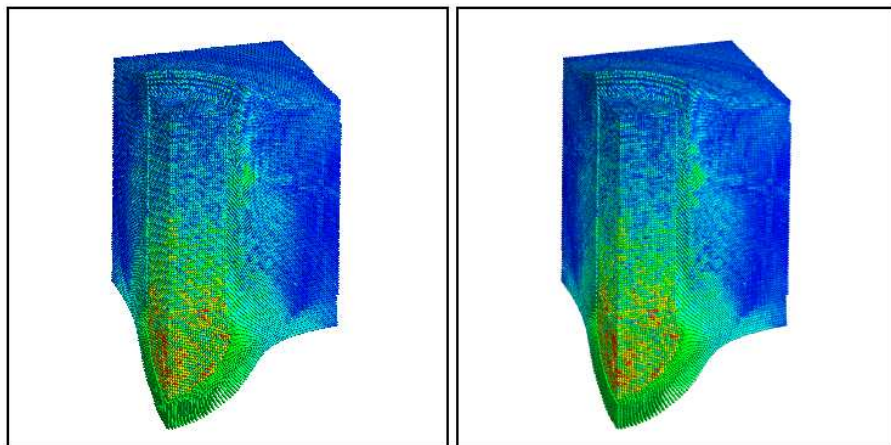


**Figure 1.3.** Aliasing can have a negative effect on the visualization process.

can provide information about proximity of structures and help disambiguate relative positions in the data[9]. However, shadows create regions where the ambient term of the shading model becomes dominate. With many local shading models the ambient term becomes constant in regions of shadow or where the surface faces away from the light source, reducing the spatial cues needed for particle visualization. Nonconstant ambient values which take into consideration global positioning become important.

# Blank Image

**Figure 1.4.** Without shadows, it is difficult to determine how far the red block is from the surface (left). Shadows can disambiguate this (center, left).

While illumination can help with shape perception, silhouette edges can be used to accentuate a set of view dependent boundaries. Our perceptual system makes use of stereo, object, and color information to distinguish boundaries[9]. While stereo is not necessary to find most boundaries, it can reinforce edge perception found by changes in color creating a stronger sense of discontinuities. Since monoscopic renderings, such as those commonly used for computer displays do not have stereo, we can augment boundaries of shapes with silhouette edges. Object based silhouette methods attempt to ascribe silhouettes to edges in the geometry. The effect of this method on particle based visualization is to accentuate the edges of each particle. This can lead to aliasing when each particle is only represented by a few pixels. The silhouette feature will be even smaller and distract from the overall representation of the data. Silhouette edges can be made more meaningful if they can provide information about the macroscopic shape represented by groups of particles.

## CHAPTER 2

### BACKGROUND

Global illumination is a lighting model which takes into consideration the placement of neighboring geometry[5]. In his paper, Kajiyama provides the definition of a rendering equation. This integral provides a model of the intensity of light from one point to another composed of the emitted light between these two points and the scattered light from the scene by the distant point all modulated by a geometric term. Simply put, this method of lighting provides not only direct illumination values, but light originating from indirect sources.

Brute force integration using Monte-Carlo integration can be used to evaluate the rendering equation, however this method is computationally expensive and is slow to converge. There have been efforts to approximate the equation to speed up computation. Greg Ward et al. used a method of caching the indirect computation to speed up neighboring pixels[13]. A ray is shot into the scene. At the intersection point a search is made of previously computed indirect lighting. If found, these values are used rather than computing the indirect lighting. This provided a significant performance boost without introducing many artifacts.

Gene Greger et al. used another method of caching illumination for later renderings[3]. They stored indirect illumination at discrete grid locations on a sphere. Objects would then use the surface normal lookup and interpolate values of nearby nodes. This approximation provided for faster renderings and slight changes in the scene. This method seems good for scenes where the grid is sufficiently resolved for the level of detail of the geometry. In the case of particle data sets generated by MPM simulations, this would not account for the fine structure.

More recently global illumination has been looked at for visualization of dynamic isosurfaces[14]. Irradiance is stored in a volume corresponding to the varying

possible isosurfaces contained in the data. When shading the extracted isosurface geometry irradiance is interpolated from nearby grid points and applied to the surface. To reduce interpolation errors, a grid of higher resolution than the data can be used for the irradiance.

While global illumination refers to the model which incorporates interreflection of light between surfaces another lighting model called ambient occlusion[7] only computes the visibility of a point with a global light source (such as a sky light source). This happens as a preprocessing phase. The amount of light reaching these points are then stored with the geometry for later use in the rendering stage. Additionally the principle direction of the incoming light can be stored to index into an environment map during rendering.

Vicinity shading is a term coined by James Stewart in his paper dealing with precomputing the uniform diffuse illumination for isosurface volumes[12]. Similar to ambient occlusion for geometry, ambient values are computed for visualizing isosurfaces generated from volumetric data. His method, however considered only the geometry in the vicinity of the surface is in the computation. Luminance is computed for a given voxel based on the visibility within a certain radius of the background giving equal weight for all directions. Surface points with more visibility had higher luminance than surfaces which were occluded by other geometry. The precomputed vicinity shading values are then stored in a separate texture volume and interpolated to the extracted isosurface during rendering. His paper showed the utility of including term based on structure of the geometry in the lighting (see Figure 2.1).

Silhouette edges are another method for enhancing shape perception of the scene. These edges are usually rendered in black and follow the view-dependent hull of the object. This helps define macroscopic structure of the geometry. Several methods [11, 2] have been proposed to compute and render these edges for polygonal scenes. One such method uses the dot product of the normal and the view direction as a lookup table into a 1D transfer function. As the dot product nears zero the surface is increasingly colored with the silhouette color. This method does not take

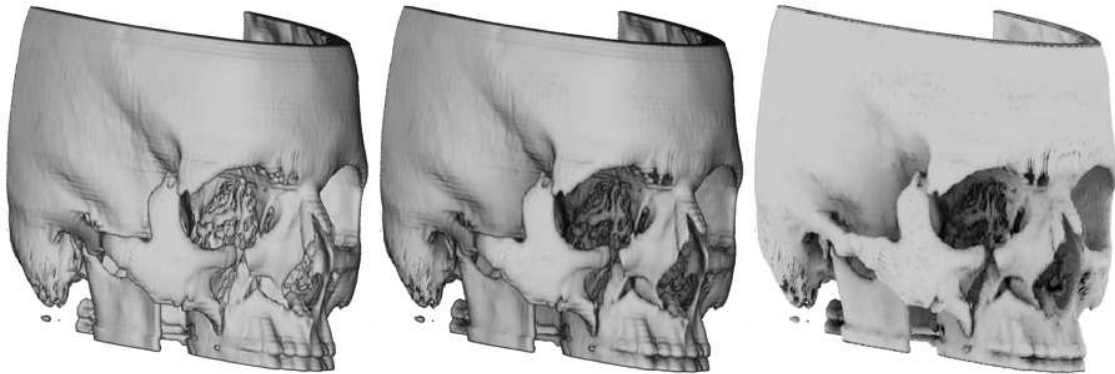


**Figure 2.1.** An isosurface representing a human skull with a fracture of bones in the right hand jaw. Vicinity shading helps the perception of space between the jaw bones and the rest of the skull. The image on the left has only phong illumination. The image on the right shows the vicinity values. The center image is the combination of the left and right images. *Image used by author's permission*

into consideration the curvature of the surface and therefore is subject to varying widths of edges. Edges on surfaces which have low curvature will have thicker silhouettes than edges where the curvature is high. Kindlmann et al.[6] addressed this issue by computing the curvature of the surface using the values in a volume to unify the edge width.

McCool used silhouette edges indirectly to compute shadows for interactive scenes [8]. His method rendered the scene from the perspective of the light and saved the depth buffer. Using this depth buffer as an image the method would perform edge detection to find discontinuities. These discontinuities, representing silhouettes, would be used to generate geometry representative of regions that were in shadow. The notable aspect of McCool's algorithm is the use of the depth buffer to generate silhouette edges.

Parker et al. provided a method to interactively view large particle data sets as spheres using interactive ray tracing and clever acceleration structures[10]. The basis for the proposed research builds on this framework. The interactive ray tracer, hereafter referred to as RTRT (Real-Time Ray-Tracer), is built of two software components.

The first implements a traditional ray tracer where rays are shot into the scene where intersections are queried. The closest objects are shaded using an assortment of material properties such as phong shading or specular reflection. Objects in the scene are stored as lists or inside specialized acceleration structures that are designed to reduce the amount of work required to find the closest object. The acceleration structure used for this work uses a hierarchical grid with the indices stored at the deepest level. Proper use of grids help reduce the number of ray/sphere intersections a ray must perform.

The second component of RTRT provides the user interface and multiprocessor framework. User input such as pan or zoom are processed and the according changes are made to the rendering system. Rendered images are displayed in a window the user can view and interact with. Because ray tracing is a per pixel operation, parallelism is achieved by assigning groups of pixels to individual threads running on their own processor. The target architecture of RTRT is large distributed memory systems such as SGI's Origin series. Once the rendering threads are finished computing the data is handed off to the display thread. The display thread displays the data in a window for the user to view.

I would talk more about particle vis, but the my literature search has turned up nothing. Use of spheres to represent particles must be so obvious that there doesn't exist papers on the topic. The only particle papers I've found use particles to trace vector flows.

## CHAPTER 3

### AMBIENT OCCLUSION

In order to investigate ambient occlusion for particle data several components have been implemented: the precomputation of values, the storage, and reconstruction during rendering. The reconstruction of the shading values occurs during rendering and is therefore performance critical.

#### 3.1 Data precomputation and storage

The framework for rendering is the interactive ray tracer developed at the University of Utah[10]. Particle visualization is accomplished by representing the particles as spheres because of the efficient ray/sphere intersection routine. Only the center and radius must be stored to perform the intersection test. The discussion of techniques to generate and apply ambient occluding shading information will pertain to spheres, since they will be used to represent particles during visualization.

##### 3.1.1 Texture Mapping

Ambient occlusion values are precomputed and stored on the surface of the geometry. In the ambient occluding papers discussed earlier, values were stored at the vertices. In Stewart's paper values were stored at voxel locations. Since spheres, however, have no natural vertices or voxels, two dimensional texture maps will be used to represent shading values on the surface. Ambient values can be precomputed and stored in these texture maps. During rendering the textures will be mapped and interpolated onto the spheres.

To apply the textures the latitude/longitude coordinate mapping commonly used for spheres will be employed (Figure 3.1). An advantage to using this mapping is the fast computation of texture coordinates used during rendering. However, a

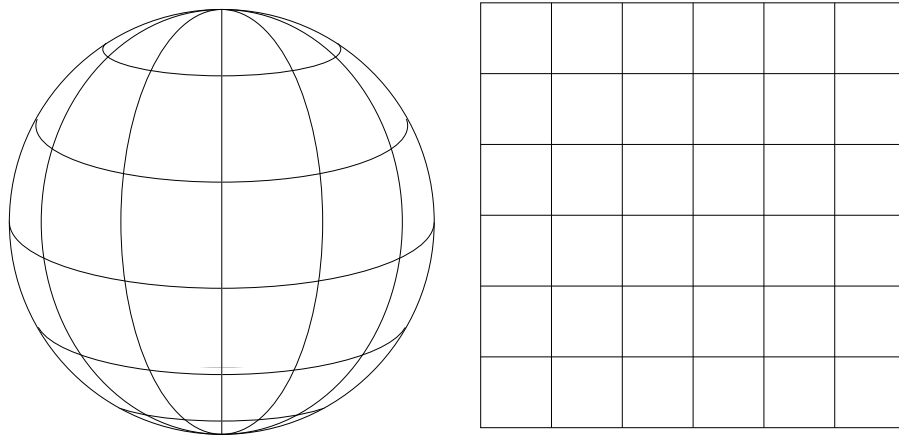


**Figure 3.1.** To texture a sphere using two a two dimensional mapping, one dimension corresponds to latitude the other to longitude.

disadvantage is that the area of the texel is non uniform. This can result in areas of greater texture refinement where the texels are small and low refinement in areas where the texels are large. In practice, however, this is only noticeable when zooming extremely close to the particles, which is not the common case. There are other mappings of two dimensional textures onto spheres that preserve area, but because texture coordinate generation during rendering of area preserving mappings can be costly, those methods were not be explored.

### 3.1.2 Ambient value computation

With the mappings established, ambient shading values can now be filled in. Particle locations are read into memory and the ray intersection acceleration structure is built. This is a modified version of a hierarchical grid with support for only spheres and the ability to crop particles based on values associated with them[10]. Precomputation time is based on the speed of ray intersections, so having a good acceleration structure is important to making this approach tractable.

Once the acceleration structure is built, computation of the shading values can begin. Ambient value textures are computed on a per sphere basis, so work can be divided among multiple processor working in parallel. Being able to generate

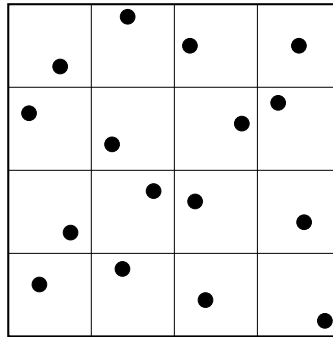


**Figure 3.2.** Jittered sampling divides the domain into regions and assigns a single point a random location for each cell.

these textures in parallel is also important to making the precomputation phase reasonable (hours instead of days).

The texture used to store the shading values is broken up into individual texels. A texture resolution of 16 by 16 texels provides a nice compromise in resolution and computation time and was used for all the images generated in this document *explain why*. Texels are sampled a user defined number of times using a jittered sampling pattern (Figure 3.2). Samples are then mapped onto the surface of the particle creating the origin for a ray.

Ray directions are generated on the hemisphere corresponding to the normal at the surface point with a cosine distribution favoring the top of the hemisphere. Using this distribution prevents having to multiply the resulting luminance by the cosine of the direction and the normal. The hemisphere sampling takes two jittered values to provide faster convergence for Monte Carlo integration.

Once the ray direction and origin have been generated a ray is shot into the geometry. If a hit occurred, then the particle is obscured from the background and no luminance is added to the texel. If no intersection occurred the texel's value is incremented by the luminance of the background corresponding to the ray.

After all the samples for a texel have been computed the value is then divided by the number of samples averaging the luminance of the background visible to the texel. This approach provides the ability to use backgrounds with non uniform luminance. Using a background with a light top and dark bottom could

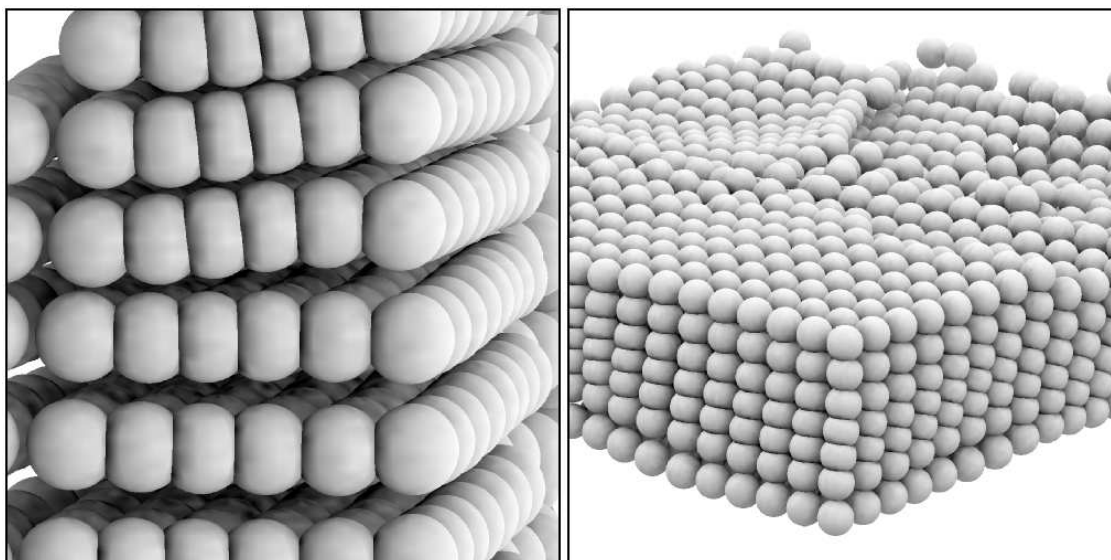


**Figure 3.3.** Bilinear interpolation can cause artifacts in regions where particles overlap. The dark banding that can be seen between the particles are caused by interpolating values that exists inside other particles with values that are outside.

add perceptual cues similar to being outside on a sunny day. When the particle's texture is finished being created, the values are dilated and written to disk for later use.

### 3.1.3 Texture dilation

Dilation of the textures are needed to compensate for errors introduced by bilinear interpolation of the texel values. This error occurs when neighboring texels are inside another particle, and hereafter referred to as being inside. Those texels not inside are conversely referred to as being outside. Texels which are inside another particle are rightly black. Through the process of bilinear interpolation these black texels incorrectly darken the areas next to this boundary. The effect can be seen in Figure 3.3 where the particles touch.

Since the texels which are causing problems are inside other particles they ordinarily do not contribute to the image. Their values can therefore be replaced by something more meaningful. By dilating values of texels outside to ones inside, these errors can be reduced significantly as seen in Figure 3.4.

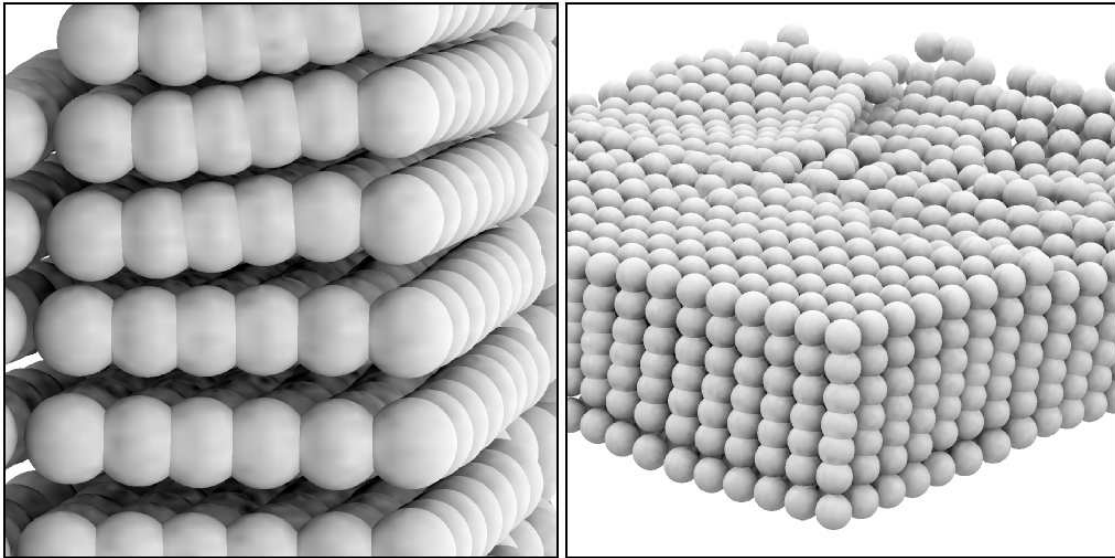


**Figure 3.4.** By dilating values that are outside to ones inside, interpolation errors can be reduced without introducing new errors.

The question becomes thus, how is a texel determined to be inside or outside? This determination is done during the ambient value computation. The geometric scene is comprised solely of spheres whose normals always face outside. When an object is intersected the normal of the intersected object is also computed. By examining the dot product of the ray's direction and the intersected object's normal we can determine which side of the object was intersected. If the inside was intersected it can be assumed that the ray originated from inside the sphere. This might not catch all cases as can be seen in Figure 3.5, but in practice some will register and be enough for the thresholding. A count is kept for how many rays from a texel were inside. This value is used later during the dilation phase to determine if a texel is inside or outside.

During a post process phase texels with an inside count above a user defined threshold are considered to be inside and are assigned an average of neighboring pixels who are considered outside.

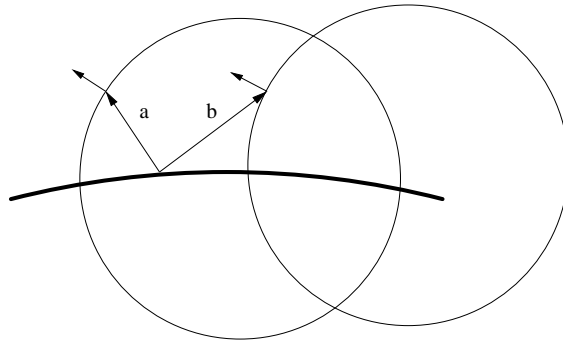


**Figure 3.5.** Determining if a ray is inside or outside by means of the dot product of the normal and ray direction works for ray  $a$ , but not for ray  $b$ .

### 3.1.4 Final post processing

After all the textures for the data set have been generated, a final post processing step is performed. This involves two methods, gamma correction and quantization to 8 bit integers. Gamma correction with a value of 2 is done to lighten up the darker regions for added perceptual acuity. Quantization is done using the maximum value in the texture set to save space in memory when the textures are needed for rendering (a cost savings of four fold). Values in the textures are computed and written to disk as floats to maintain a reasonable precision for post processing operations, however rendering does not require this precision and 8 bits per texel is sufficient.

## 3.2 Render phase

The particle data and texture data is read in to memory. The previously mentioned acceleration structure is built and used to perform ray object intersections. Once a particle has been intersected its number is used to index the textures in memory. The textures are in the same order as the particles, so that during this phase the appropriate texture can be used.

The intersection point and center of the sphere is used to calculate UV coordinates in the same manor as during texture generation to ensure the proper correlation. These coordinates are then used to lookup texels. Bilinear interpolation is used to give the textures a more smooth appearance than nearest neighbors would

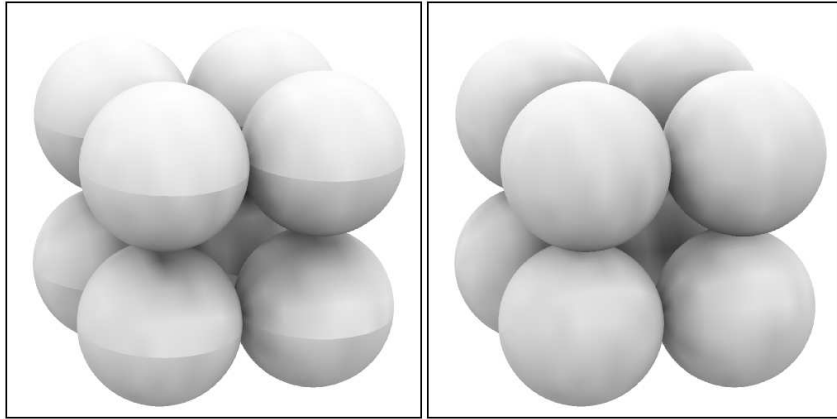


**Figure 3.6.** By wrapping the textures across the U parameter the seam can be eliminated.

provide. Texels are wrapped along the latitude direction of the texture, but not the longitudinal. This helps eliminate the seam running down the side as seen in Figure 3.6.

### 3.3 Analysis

#### 3.3.1 Precomputation Time

While precomputation time is not the focus of this research, an examination of the computational expense is provided. Precomputation time is based on the number of total samples in the scene multiplied by the average intersection time. The number of total samples is the product of the number of samples per texel, texels per sphere, and spheres themselves. Table 3.1 lists some approximate times for texture generation.

The difference in rendering times for data sets with relatively equal number of particles is due to the placement of particles. With MPM, particles start with an even distribution. As the simulation progresses the particles move about creating regions of higher and lower densities. Grid based acceleration structures favor geometry of even distribution (provided the objects are of similar size).

While these precomputation times can be quite expensive, they are reasonable provided the availability of large parallel hardware. Whether or not the computa-

**Table 3.1.** Approximate time to generate textures for varying data sets. All times given are for 49 samples per texel with 16x16 (256) texels per sphere (12544 samples per sphere). Computation was done using 20 processors on an SGI Origin 3800 with 600 MHz R14K processors. Images using the textures are also referenced.

Name	Figure	Number of particles	Total number of samples	Time to generate
Fireball 6	3.7	955,000	11,979,520,000	66 min.
Fireball 11	3.8	952,755	11,951,358,720	261 min.
Cylinder 6	3.9	214,036	2,684,867,584	13 min.
Cylinder 22	3.10	212,980	2,671,621,120	25 min.
Bullet 2	3.11	569,523	7,144,096,512	35 min.
Bullet 12	3.12	543,088	6,812,495,872	33 min.
Foam 50	5.1	7,157,720	89,786,439,680	12 hours

tion cost can be amortized by the benefit to the visualization is not the focus of this research. Precomputation time can be reduced by either creating better performing ray intersection code or by decreasing the number of samples.

### 3.3.2 Impact on rendering time and memory

In order to make sure we keep the renderings interactive the ambient occlusion values must be precomputed. Fifty samples per pixel would have too much of an impact on frame rates. Even a factor of ten would be unacceptable reduction in performance. The ambient values are therefore stored in a texture. The impact on memory usage is directly related to the resolution of the textures used. A single texture is then stored for each particle. Textures have only a single byte per texels representing the ambient value. If a the resolution of a texture is 16x16, as in the images displayed in this text, each sphere would need 256 bytes. The memory requirements for a series of data sets can be found in Table 3.2.

Since interactivity is the goal of preprocessing and storing all the textures, the effect on frame rates must also be addressed. In Table 3.3 relative frame rates for various data sets and view are shown. Using the ambient occlusion values does

**Table 3.2.** Extra memory required to store the ambient value textures for various data sets.

Name	Figure	Number of particles	Texture memory (Bytes)	
Fireball 6	3.7	955,000	244,480,000	233 GB
Cylinder 22	3.10	212,980	54,522,880	52 GB
Bullet 2	3.11	569,523	145,797,888	139 GB
Foam 50	5.1	7157720	1,832,376,320	1,747 GB

**Table 3.3.** Relative frame rates for a series of views and data sets. Computation was done using 20 processors on an SGI Origin 3800 with 600 MHz R14K processors. The image rendered was 500x500 pixels except Bullet 2 and Bullet 12 which were 250x500 to match the images.

Name	Figure	Without textures (f/s)	With textures	Textures without direct lighting
Fireball 6	3.7.A	18.96 f/s	17.23 f/s	19.10 f/s
Fireball 6	3.7.C	13.89 f/s	12.70 f/s	14.40 f/s
Fireball 11	3.8.A	12.00 f/s	10.68 f/s	10.86 f/s
Fireball 11	3.8.C	9.09 f/s	8.49 f/s	9.45 f/s
Cylinder 6	3.9.A	16.77 f/s	15.07 f/s	16.47 f/s
Cylinder 6	3.9.B	9.86 f/s	9.23 f/s	10.26 f/s
Cylinder 22	3.10.A	15.22 f/s	14.04 f/s	15.14 f/s
Cylinder 22	3.10.B	8.19 f/s	7.84 f/s	8.35 f/s
Bullet 2	3.11.A	29.90 f/s	26.67 f/s	30.01 f/s
Bullet 2	3.11.C	26.43 f/s	24.50 f/s	27.56 f/s
Bullet 12	3.12.A	32.89 f/s	28.75 f/s	30.50 f/s
Bullet 12	3.12.C	24.62 f/s	22.66 f/s	26.32 f/s

increase rendering times, however the impact is only about 10%. This is quite reasonable.

The last column of the table shows the frame rates using the ambient textures, but without the direct lighting computation. The textures provide some variance in lighting over the surface, and can be used without the addition of the direct lighting. The disadvantage of this would be the inability to use shadows, as this

requires adding the direct lighting component when a surface is not in shadow. As can be seen in the table, using only the ambient occlusion values can provide frame rates as good as or better than using only direct lighting. In many cases this can be preferable when direct lighting is not needed for shadows.

### 3.3.3 Perceptual results

By computing ambient occlusion values, global information can be encoded in the texture. This information is unique to each particle and gives a much better impression of the shape of the structure than without it. Figure 3.13 shows an MPM data set with and without the ambient occlusion shading.

One benefit of computing only the ambient term is the ability to combine it with other lighting techniques such as shadows at rendering time. This provides the ability to dynamically change the lighting conditions used for direct lighting conditions to suit the needs of the visualization.

Another option for shadow or other direct lighting generation is to compute them when the textures are generated. This requires selecting a location for the light as well as an intensity that balances the light's contribution with the ambient values in the scene. If the light is made too bright, the ambient values will be too dark. Only the ambient values can be seen if the light is too dark. However, one benefit of computing the shadows as a preprocess is the computation savings of not having to shoot shadow rays during rendering. The savings here depends on the complexity of the geometry, however since the rendering cost is independent of the content of the texture there is no additional rendering cost to include shadows in the textures.

One of the benefits of visualizing particle data sets with an interactive ray tracer is the ability to crop particles based on their value. This is an invaluable tool for domain scientist who wish to view different aspects of their data. The most common use is to crop the values based on physical location to view the inside structure. Since ambient occlusion shading is inexorably tied to the physical presence of all the particles, the shading no longer holds. Figure 3.14 and 3.15 illustrates this problem.

However, once a suitable cropping is obtained the ambient occlusion information can be recalculated.

The use of ambient occlusion shading can greatly augment the perception of structure during visualization and is therefore appropriate. The ability of domain scientists to use it without having to tune rendering parameters is also beneficial. Precomputation time is tractable, however it can be a deterrent for use. The memory requirements to store the textures will reduce the number of time steps that are possible to load into memory, a feature that makes viewing time varying data in RTRT desirable. The impact of using the textures on frame rates, however, are minimal and provide the same level of interactivity as without using them.

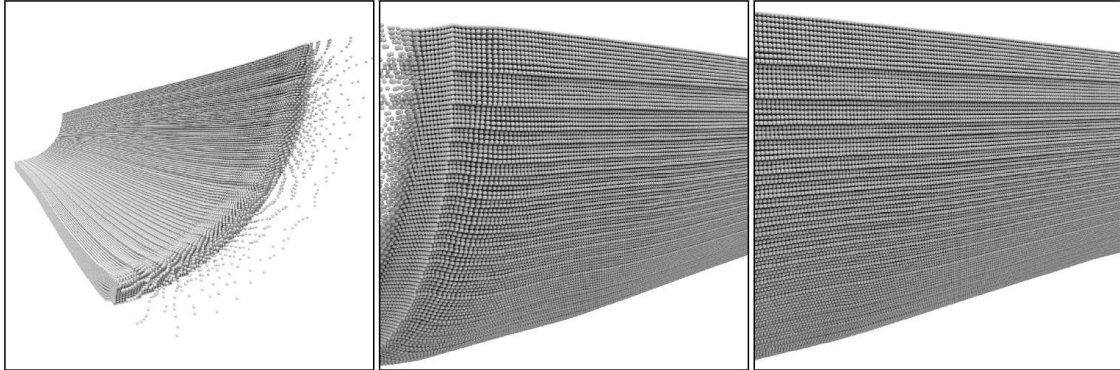


**Figure 3.7.** Ambient occlusion shading texture values mapped on the Fireball 11 data set. The views are identical to the ones in Figure 3.8. Sub-images are referred to as A, B, and C, left to right.

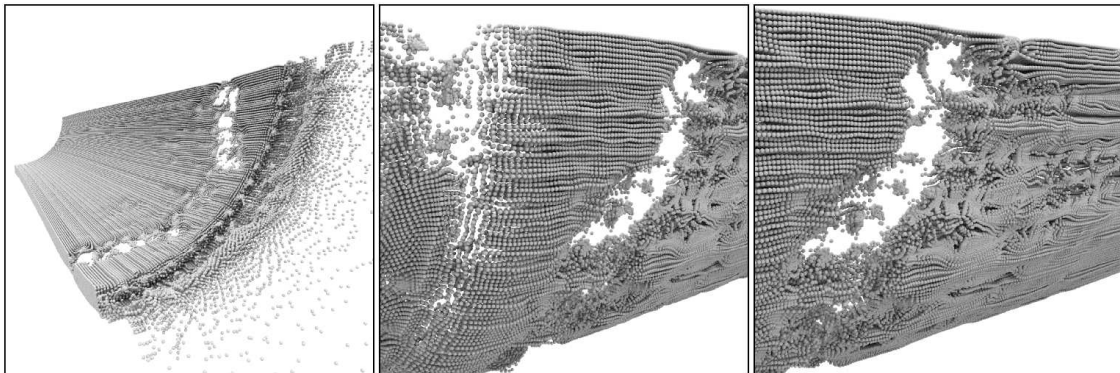


**Figure 3.8.** Ambient occlusion shading texture values mapped on the Fireball 11 data set. The views are identical to the ones in Figure 3.7. Sub-images are referred to as A, B, and C, left to right.

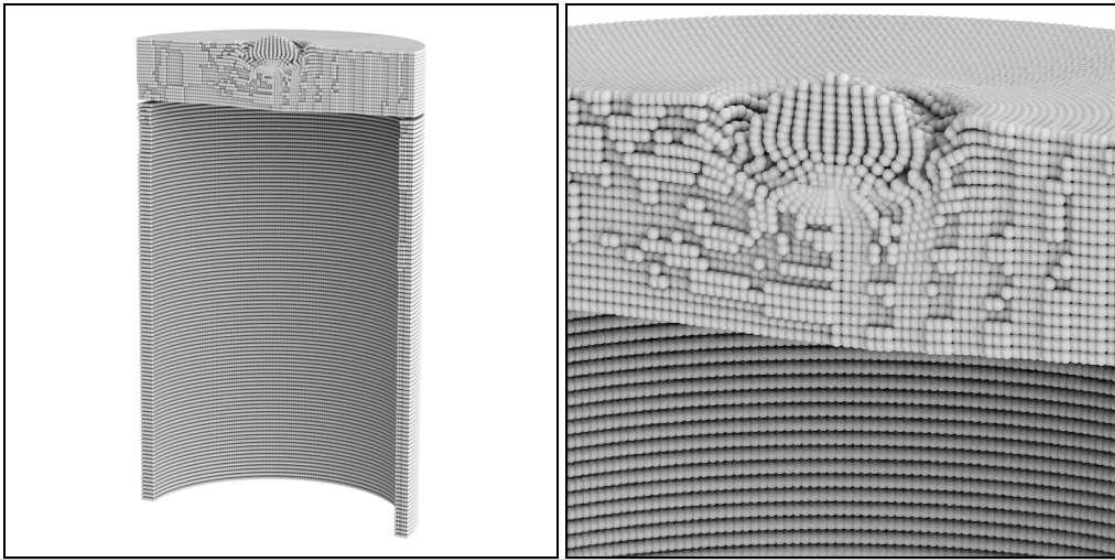


**Figure 3.9.** Ambient occlusion shading texture values mapped on the Cylinder 06 data set. Notice how the intricate structure is quite visible on the center of the structure. The spheres that protrude further from the front surface are clearly seen to do so. The views are identical to the ones in Figure 3.10. Sub-images are referred to as A (left) and B (right).

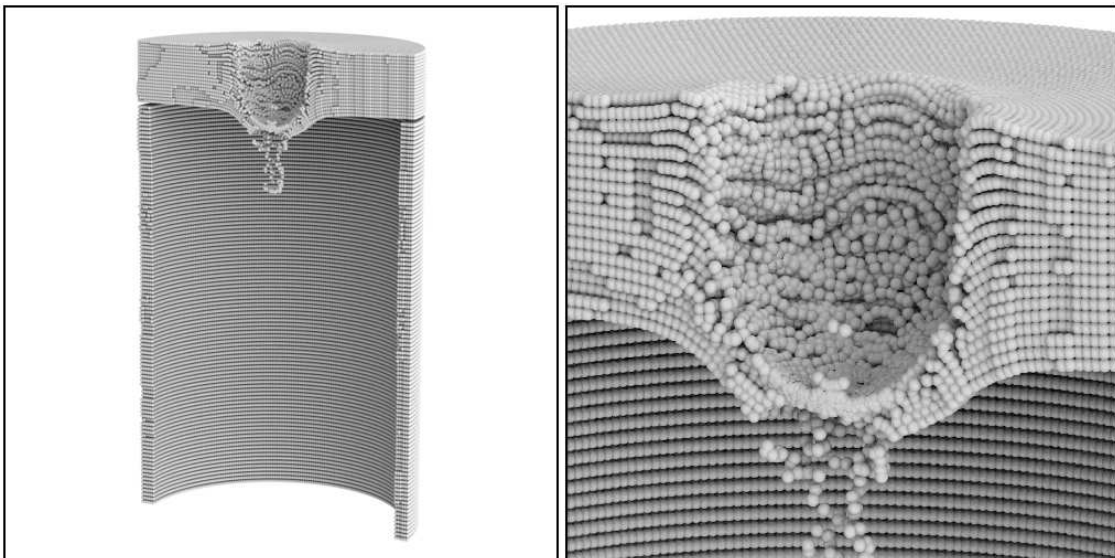


**Figure 3.10.** Ambient occlusion shading texture values mapped on the Cylinder 06 data set. One thing to note is the ability to see the two spheres standing out in front of the hole. The views are identical to the ones in Figure 3.9. Sub-images are referred to as A (left) and B (right).

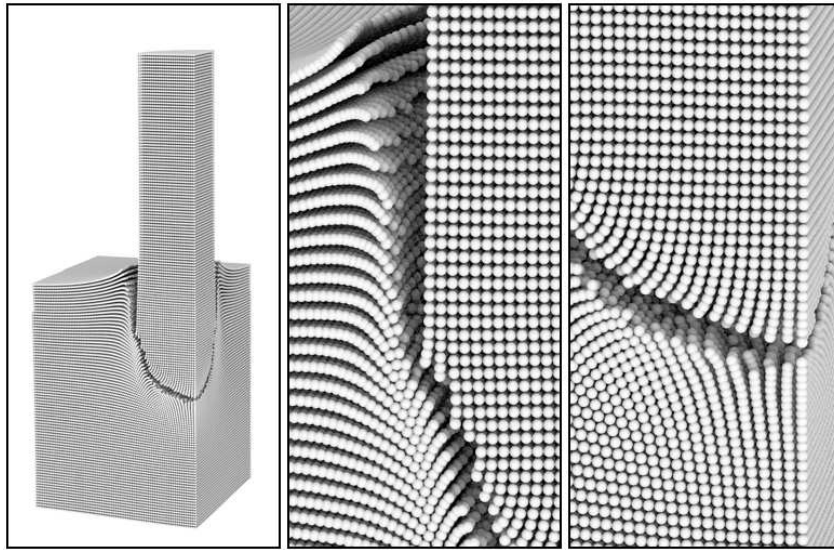


**Figure 3.11.** Ambient occlusion shading texture values mapped on the Bullet 02 data set. Sub-images are referred to as A, B, and C, left to right. Figure A provides a view of the whole data set, while B and C show some close ups. The relative positions of the bullet with the material are easily perceived. The views are identical to the ones in Figure 3.12.

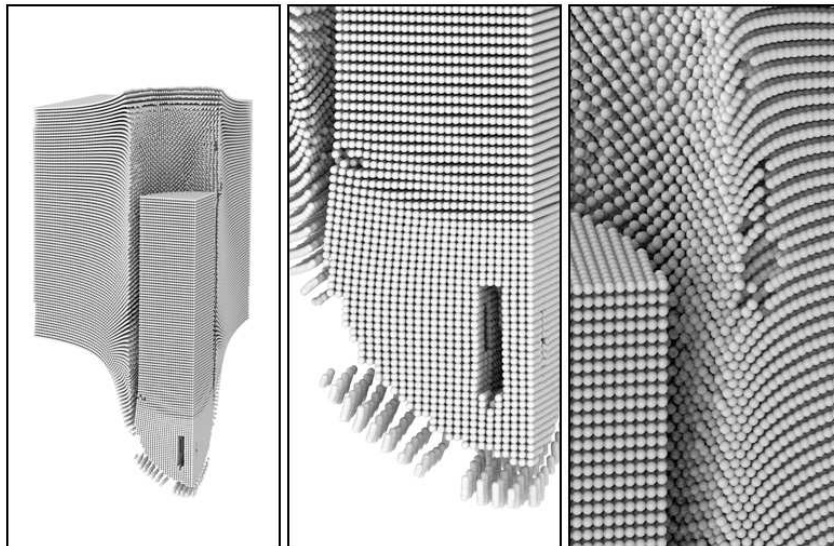


**Figure 3.12.** Ambient occlusion shading texture values mapped on the Bullet 02 data set. Sub-images are referred to as A, B, and C, left to right. Figure A provides a view of the whole data set, while B and C show some close ups. As with Figure 3.11, the relative positions of the bullet with the material as well as inside the holes in the objects are easily perceived. The views are identical to the ones in Figure 3.11.

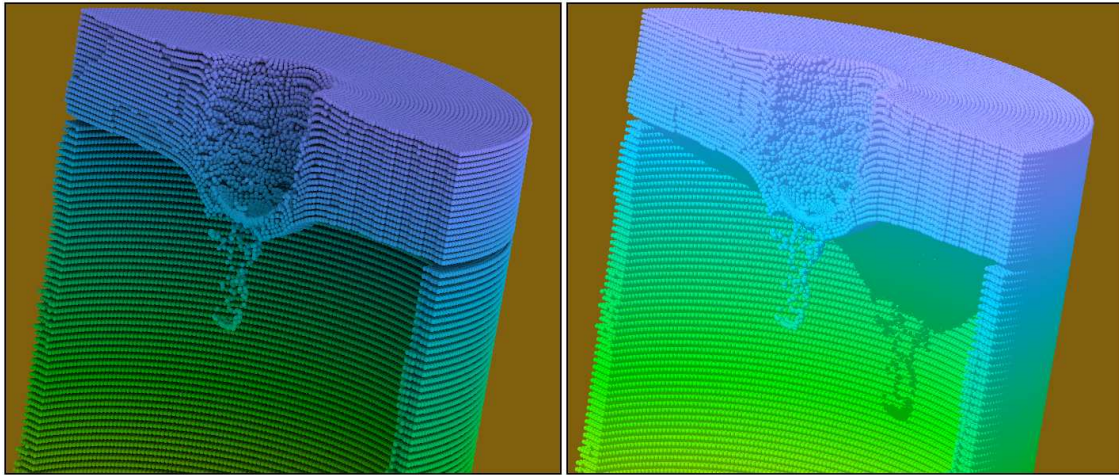


**Figure 3.13.** The image on the left is without ambient occlusion information. The one on the right includes the ambient shading.

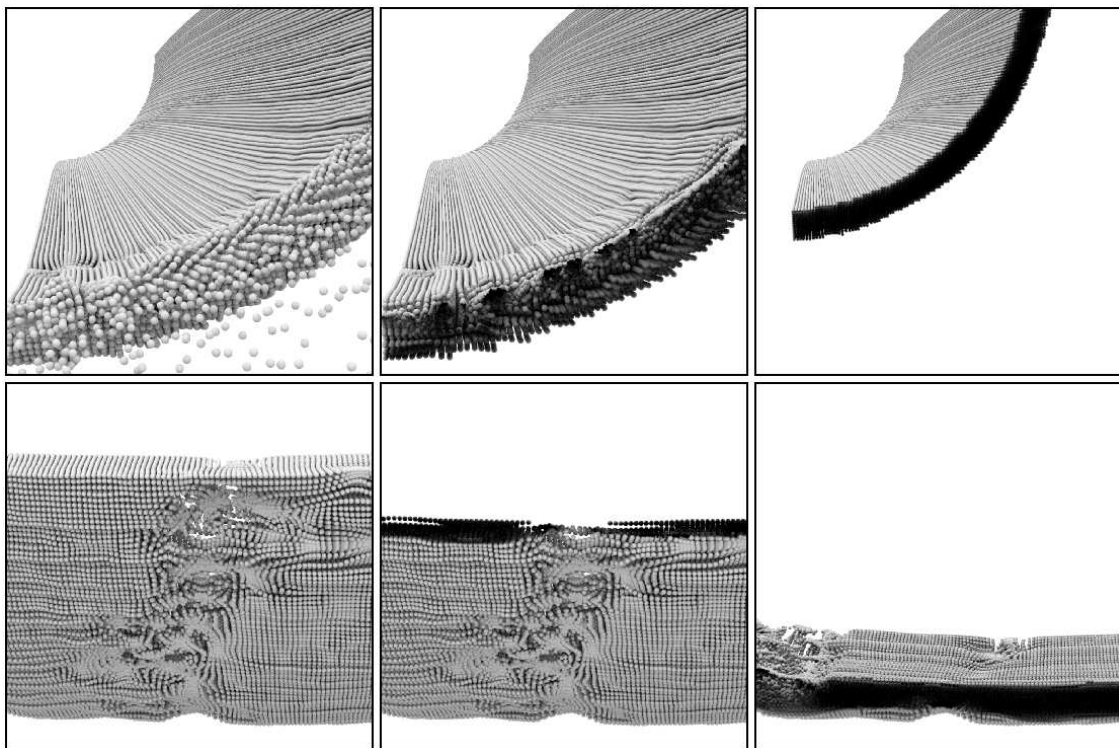


**Figure 3.14.** As the data is cropped, the ambient occlusion shading values are no longer applicable. The far left images show the uncropped data set. The center and right images show progressive cropping of the data. The internal particles that were not visible before the cropping are erroneously dark.

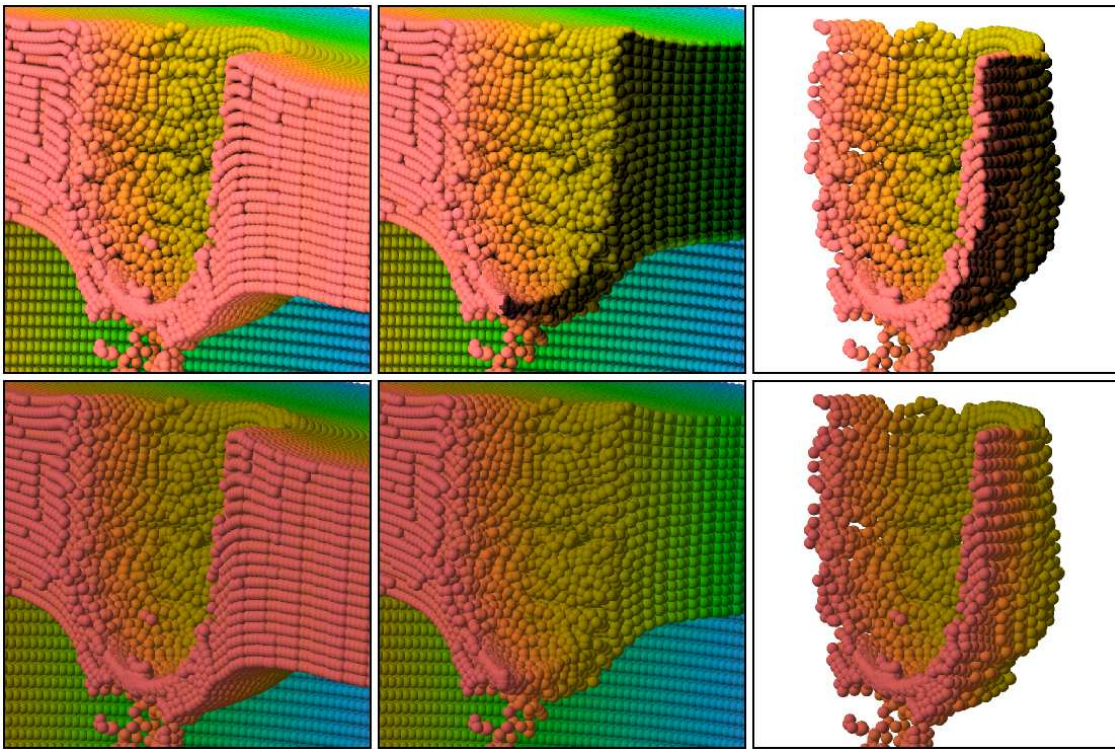


**Figure 3.15.** The images above show the visualization with the ambient occlusion values combined with direct lighting. The lower images use only the direct lighting contribution. The image on the left is the uncropped data. Images in the center and right hand sides show two different croppings.

## CHAPTER 4

### SILHOUETTES

Structures found in data sets generated using the material point method are generally represented using groups of particles. Silhouette edges placed on the edges of these structures can help to accentuate them. Since the macroscopic structures are made up of individual sphere object based methods would need to account for the groups of particles and compute them as a preprocess.

An image based approach could be object agnostic as well as eliminate the preprocessing phase. Using a depth buffer as an image, edge detection can show where there are discontinuities in depth and thus, geometry. These edges can be used to place the silhouettes on the image during rendering.

In order to perform images based silhouette edges, the depth buffer must be stored, edge detection performed, and edges applied to the final rendering.

#### 4.1 Depth buffer from ray tracing

Ray tracing determines the closest object by comparing intersection points along a ray  $f(t) = direction * t + origin$ . Comparisons are done using values of  $t$ , and the object corresponding to the smallest value of  $t$  is treated as the closest object. If the direction vector used is normalized, the units of  $t$  between pixels are uniform and can be used in operations together. The values of  $t$  for each pixel can be thought of as a depth value, the collection of all  $t$ 's as a depth buffer. While the depth buffer does not need to be explicitly stored during the process of generating the ray traced image, the information is already computed as part of the ray tracing process and can be cached for later use. Figure 4.1 shows an example of the depth buffer and image used to generate it.

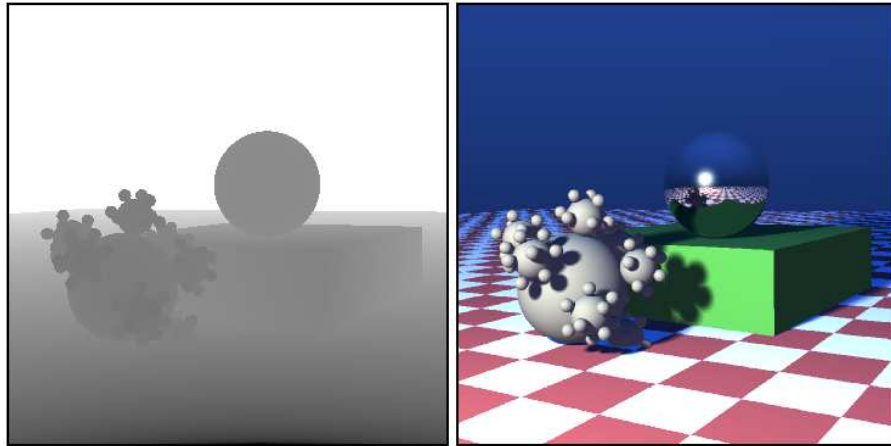


**Figure 4.1.** The depth buffer and the corresponding image generated using RTRT. The values for the depth buffer have been quantize in such a way as to make the foreground discontinuities more visible.

## 4.2 Generating silhouette edges from the depth buffer

A popular method of computing edges in images is using the Laplacian of a Gaussian (LoG). This kernel is convolved with the image and edges are marked where there are zero crossings. The Gaussian is used to smooth the image first, because, as a second derivative kernel, the Laplacian is very sensitive to noise (see Figure 4.2). However, because the depth buffer is already relatively smooth, convolution of the Gaussian is unnecessary. Therefore, only the Laplacian is needed to look for zero crossings in the second derivative. In the implementation used for this thesis it is done using a 3x3 kernel of the shape found in figure 4.3.

Zero crossings are discovered by taking the difference between the center sample and the remaining surrounding samples. Since all depth values are positive, non zero differences indicate a zero crossing or an edge. One thing to take into consideration are double edges produced where there are discontinuities in the first derivative. To prevent these double lines only differences which are positive are taken into account (see Figure 4.4).

Marking all the silhouette edges in an image can be desirable in some cases as can be seen in Figures 4.5 and 4.6. Here the silhouettes provide a trend in particle

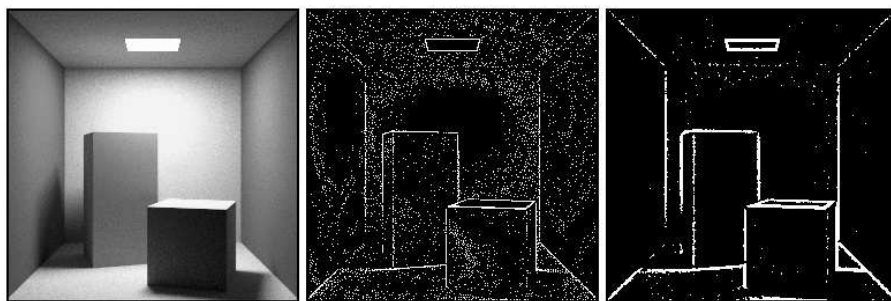


**Figure 4.2.** Second derivative kernels are very sensitive to noise, and usually require smoothing the input first to produce reasonable results. The image on the left is the original image. The center image is made by thresholding the Laplacian without any smoothing. The right side image smooths the image using a Gaussian, convolves with the Laplacian, and thresholds the values.

-1	-1	-1
-1	8	-1
-1	-1	-1

**Figure 4.3.** Laplacian Kernel

placement where lighting does not show the individual particles well or where the particles are in shadow and the spheres' color is constant.

Other cases this may result in too many silhouettes cluttering the image or generating aliasing (see Figure 4.7). To reduce the number of silhouettes, we must have a way of marking those edges which are of more importance. For our application the edges of more importance are those with higher discontinuities in depth. Using the magnitude of the Laplacian we can mark edges where the discontinuity is greater than a threshold. By varying this threshold we can selectively show edges corresponding to different degrees of discontinuity. Figure 4.7 shows a series of images where silhouettes are drawn for edges of increasing discontinuity.

The threshold can be used while rotation the object or changing the field of view without needing updating under certain circumstances. When the silhouettes are using the depth threshold, this threshold is only meaningful and useful while the image changes if the relative depth of the particles in the scene remain relatively

constant. Conditions which provide this are common. Typical renderings of these particle datasets keep the look at and focal point at the center of the object. A user will usually only rotate the object or change the field of view, keeping the relative depth values meaningful to the depth threshold.

In RTRT edge detection is done after the image is finished rendering, because we cannot guarantee neighbor information availability until after all rendering threads are finished computing their pixels. Only a single pass is necessary to do the edge computation, as the Laplacian is computed for each pixel and edges assigned based on the threshold.

### 4.3 Analysis

One advantage of the silhouette edges is the precomputation time. Since the method described in this thesis is entirely image based, no precomputation is necessary. However it does require computation while rendering. For our particular implementation edge detection is done in a separate thread from the image rendering, and the computation is faster than the rendering threads and does not impact rendering time. Table 4.1 show the relative performance when computing silhouette edges while running.

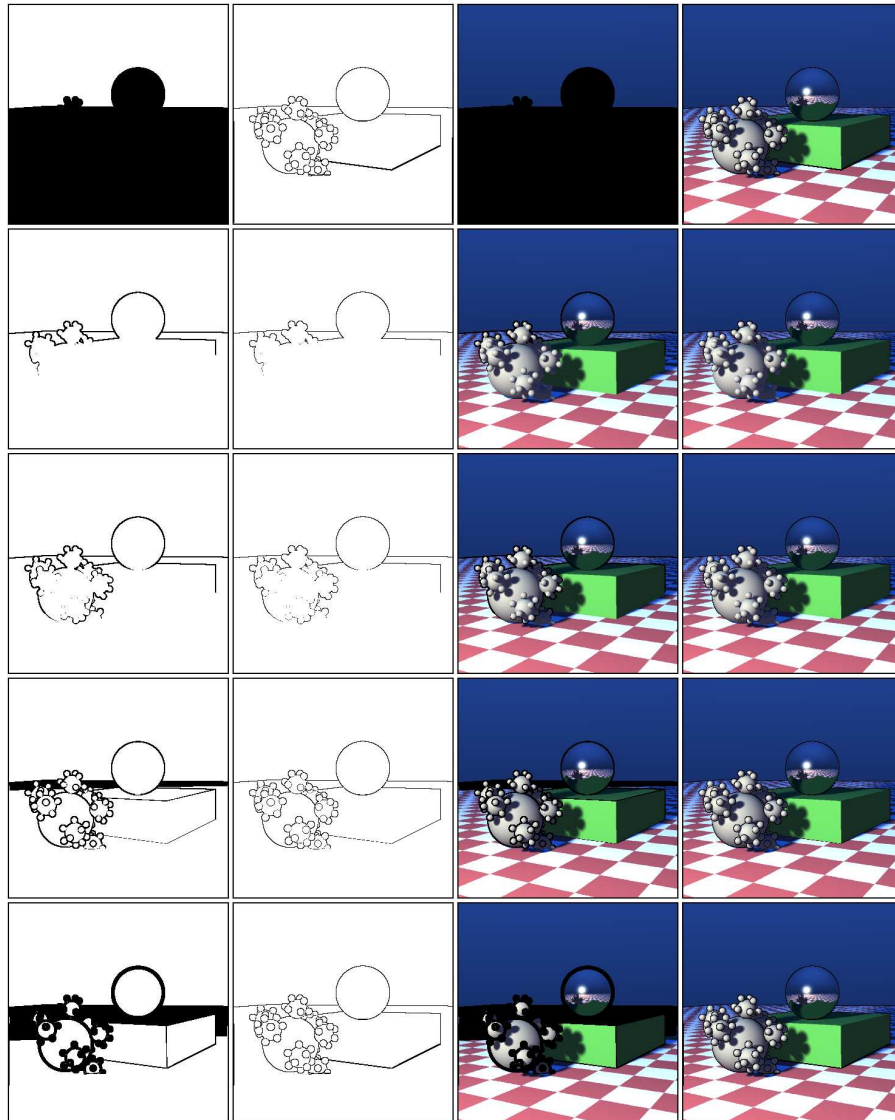
**Table 4.1.** Relative frame rates for a series of views and data sets. Computation was done using 20 processors on an SGI Origin 3800 with 600 MHz R14K processors. The resolution of the images rendered is 500x500 pixels.

Figure	Without Silhouettes (f/s)	With Silhouettes
Figure 4.1.B	17.064 f/s	16.056 f/s
Figure 4.7.C	2.220 f/s	2.179 f/s
Figure 4.7.B	2.220 f/s	2.197 f/s
Figure 4.8.A and 4.8.B	1.155 f/s	1.162 f/s
Figure 4.8.C and 4.8.D	2.683 f/s	2.632 f/s

The impact on memory is based on the resolution of the image. Since the depth buffer is now stored, an extra four bytes per pixel are required to store the depth.

The image buffer also uses four bytes per pixel to store rendering results (one byte for red, green, blue, and alpha channels). Windows typically used for rendering contain 40,000 to 360,000 pixels (200x200 to 600x600). At four bytes per pixel, the overhead to store the depth buffer ranges from a hundred kilobytes to two megabytes. On modern distributed shared memory systems, typically containing gigabytes of memory, the memory impact is very small.

Based on the experiments done, the use of silhouette edges is appropriate applied to particle data sets of this nature. Users can make use of it immediately during their renderings and with the help of the user defined threshold, can have a device to aid in the visualization process.



**Figure 4.4.** The left most column contain images where the edges are assigned by using the absolute value of the Laplacian compared with a threshold. The second column from the left is where only the positive values of the Laplacian are greater than a threshold. The right two columns of images show the edges applied to the rendered image. The top row of images compare the Laplacian to a threshold of 0, while the lower images use progressively smaller and smaller thresholds encompassing more and more edges.

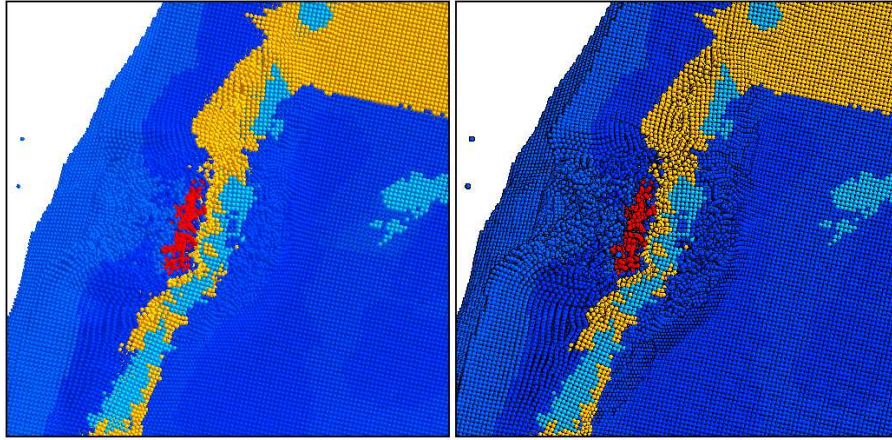


**Figure 4.5.** Silhouettes over each particle can be useful showing trends in particle placement, especially without shadows

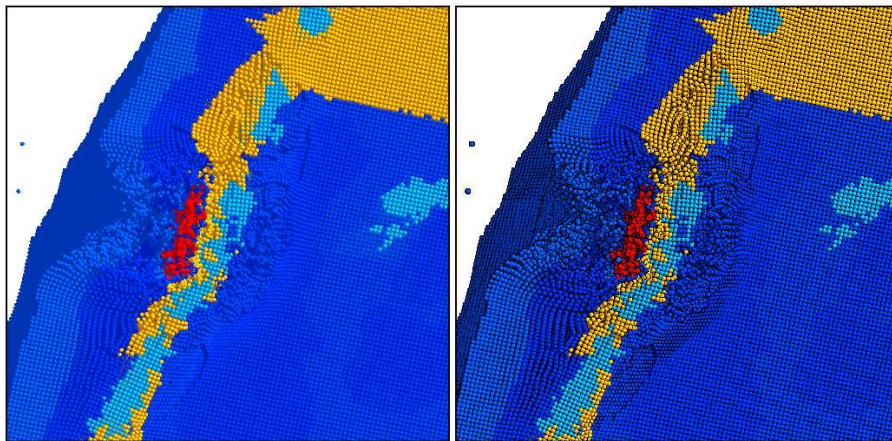


**Figure 4.6.** The same data and view as Figure 4.5, but with shadows

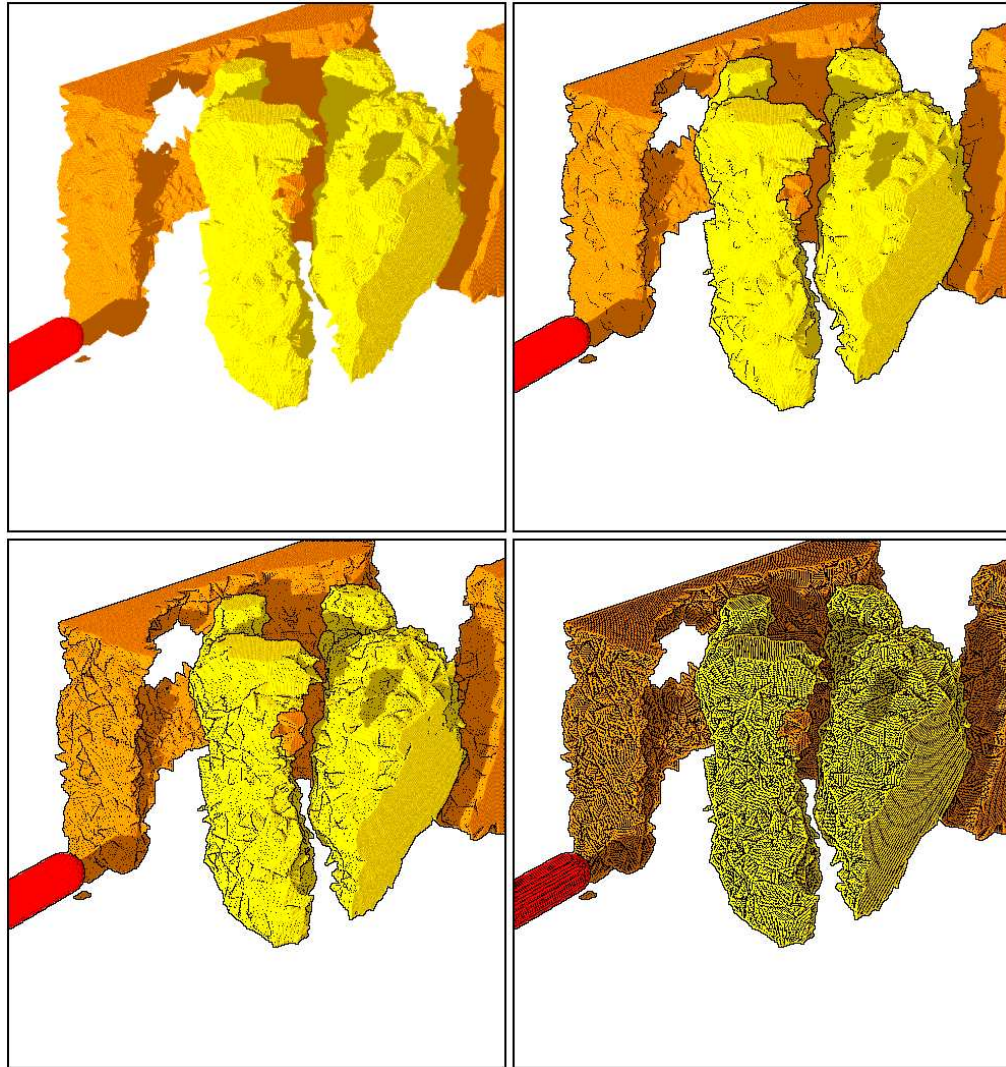


**Figure 4.7.** By varying the threshold of the Laplacian to be counted as an edge we can change how many edges are displayed. The upper left image shows no silhouettes. The upper right and lower left show progressively more and more edges. The lower right image, shows all the detectable edges.

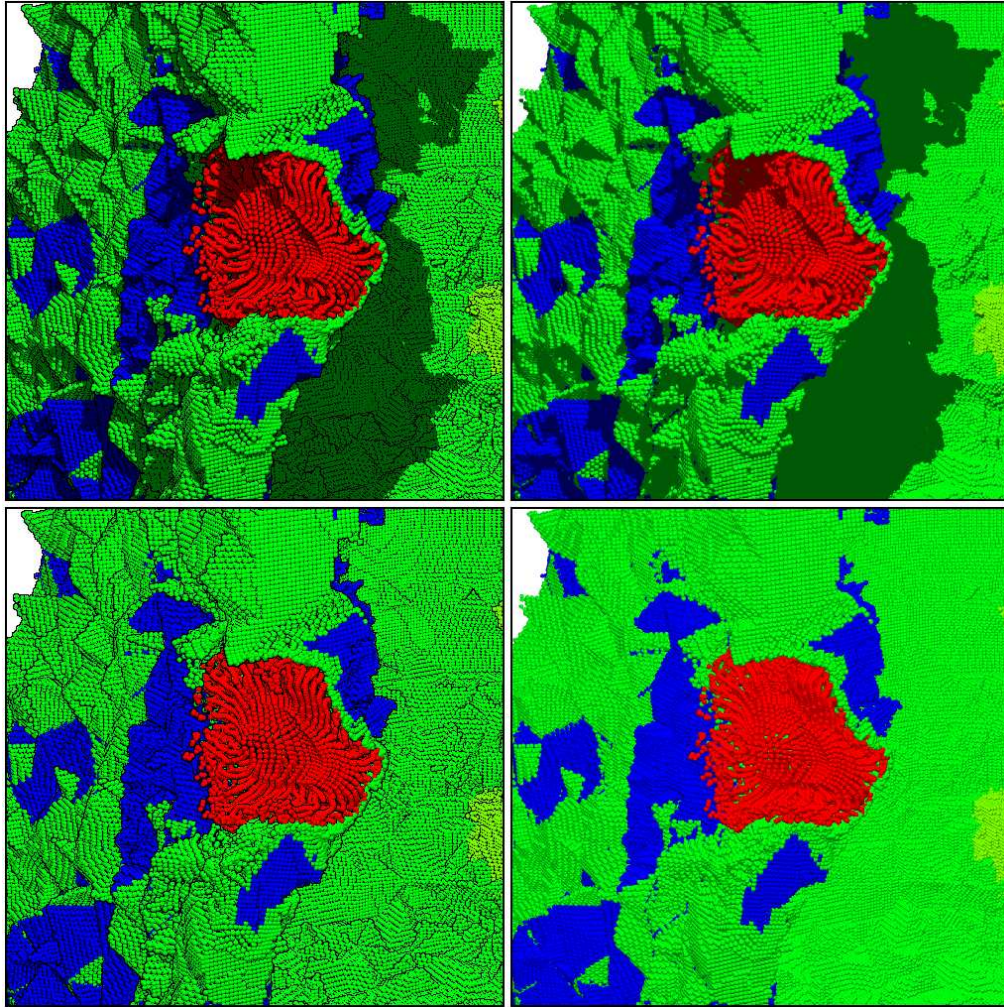


**Figure 4.8.** These images show the use of silhouette edges with and without shadows. The images are referred to as A (top left), B (top right), C (bottom left), and D (bottom right). Images on the top have shadows, while images on the left have silhouette edges.

## CHAPTER 5

### CONCLUSIONS AND FUTURE WORK

The goal of this thesis was to ascertain the appropriateness of the use of ambient occlusion and silhouette edges for particle visualization. Appropriateness can be defined as both the affected quality of the visualization and the feasibility of the use of these systems.

#### 5.1 Ambient Occlusion

Ambient occlusion provides global lighting information that can be viewed interactively. This information is purely used for spatial perception. Domain scientists who were consulted stated the visualization with ambient occlusion value textures was of benefit to them, but only if they could be used for time varying data. Since RTRT provides these scientists the ability to view many time steps each containing hundred of thousands to millions of particles interactively, having textures for all the particles in memory would be necessary.

There are two major obstacles for this to occur. The first is the amount of memory required to store the textures in memory. Since 256 bytes are required for each particle that itself only takes twelve or more bytes, only about a tenth the number of time steps can be loaded into memory. There may be, however, ways to overcome this that could be investigated for future work. The resolution of the texture could be reduced. What would the results look like with lower resolutions? How good would it look with only a single ambient value per sphere?

Another way to relieve the memory burden is by reducing the number of textures in memory. This could be done several ways. First, the textures could be compressed in such a way as to take advantage of the redundancy in the texture sampling. One such form of redundancy is completely black textures corresponding

to many particles that lie inside a group of particles completely obscuring the background. This and other redundancy could perhaps be exploited for significant gains. Second, memory for textures could be demand paged, so only the textures of the visible particles are loading into memory. Third, textures could have a variable sizes, based on the variation in the texture. Textures with lower variation would be represented with fewer texels.

The other factor limiting the usefulness of ambient occlusion textures is the precomputation time. Even utilizing multiple processors running in parallel, pre-computation time could take anywhere from 30 minutes per time step to several hours. The foam data set, as seen in Figure 5.1 and consisting of 7.1 million particles, took 12 hours to compute the textures using 20 processors on an SGI Origin 3800. While the preprocessing time is acceptable for creating nice visualizations for a small number of time steps, it quickly becomes intractable for large number of them.

The problem of precomputation time could be addressed in several ways. The first is to reduce the number of texels used in a texture, either uniformly or on a texture by texture basis as described above. A second way is to use a smaller radius for occlusion queries. Currently the ray must reach the extents of the geometry without registering a hit before it is deemed to have no occlusions. Perhaps, similar to Stewart's paper, a vicinity query could be computed. This would reduce the radius for occlusion queries and result in earlier ray termination. The radius would be a user defined parameter. The performance benefit and impact on spatial perception would have to be investigated as future work. Further work could be done to improve the efficiencies of the ray intersection routine. Since this is the most time consuming portion of the precomputation time, reducing the cost of performing ray intersections will decrease texture generation time. Another way to reduce the precomputation cost is to only generate textures that are visible by performing view dependent queries. During an interactive phase, texels viewable from the rendering can be flagged for later precomputation. This will reduce the number of generated texels which would not be visible anyway.

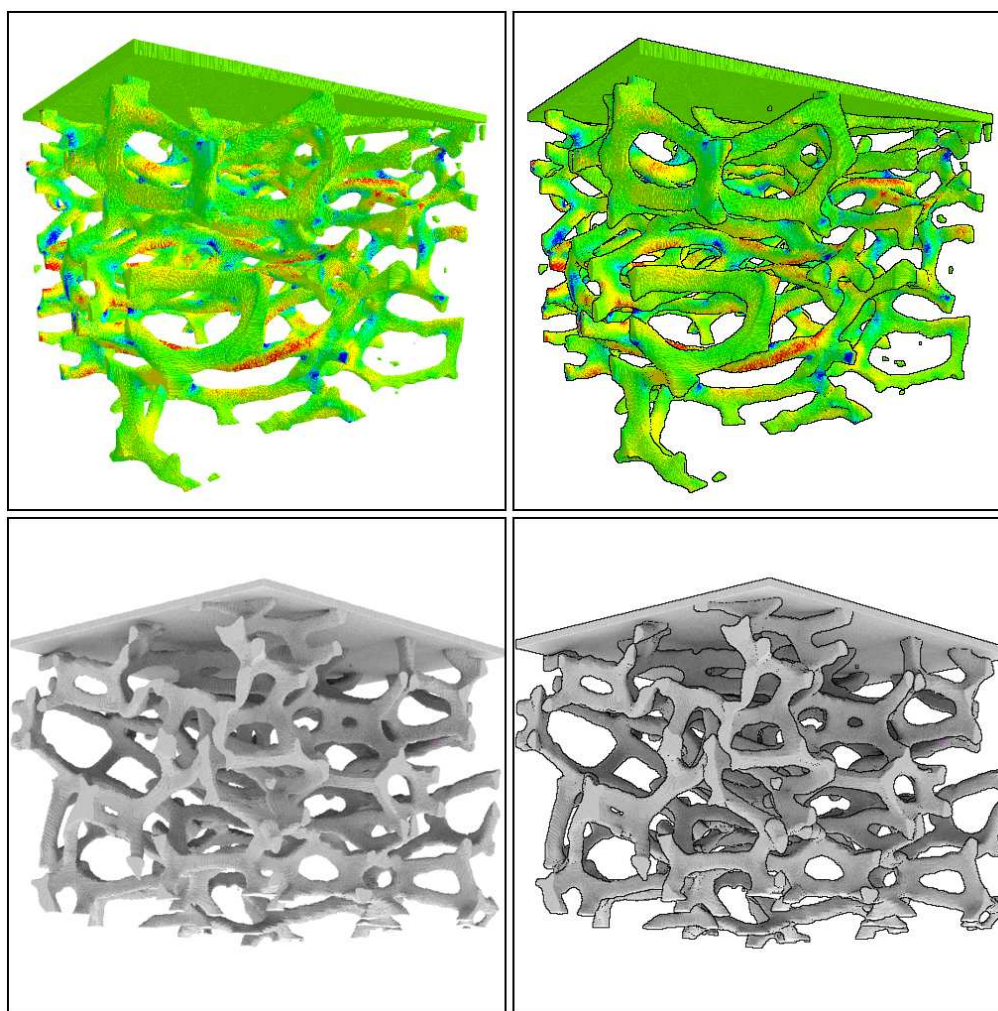


**Figure 5.1.** This data depicts a foam structure being crushed. The top images are with direct lighting only with color mapping. The bottom images show the ambient occlusion values applied to the data set. Images on the right contain silhouette edges, the ones on the left do not.

The domain scientists need to be able color map their data. The use of ambient occlusion textures does not interfere with the ability to color map the particles as can be seen in Figures 3.13 and 3.15. Another feature user took advantage of is the ability to use shadows to accentuate various features. Since the ambient textures do not include direct lighting information, any component of the direct lighting such as the position of the light, its intensity, or color can be changed as need be for the purposes of the visualization.

One feature domain scientists use when visualizing their particle data sets is the ability to crop out particles based on values associated with the particles. This feature allows the user to view only the parts of the data that are of interest. When particles are cropped, the values in the ambient occlusion textures no longer correspond to the visualization being viewed. User could recompute the texture values with the new cropping, but this can take much longer than the investigative process of visualization reducing the ability to explore the data freely. A method to dynamically update the particles would need to be developed to overcome this issue. If a visibility query is made on the initial data and stored, this data could be used to recognize newly visible particles and dynamically update the shading on those particles and perhaps those in the neighborhood. This would reduce the cost of recomputing the entire thing. Adaptive methods such as these would still be costly and could lead to potential errors when textures do not correctly correspond to the viewable geometry. For now this method is limited to static and fly through visualizations, and not dynamic exploration.

In reference to the quality of the visualization, domain scientists indicated they liked the look of the visualization. However, the precomputation time and memory constraints were deterrents.

## 5.2 Silhouette edges

The other focus of this thesis was the appropriateness of silhouette edges. The use of silhouettes has several benefits, no precomputation time, little impact on frame rates, intuitive user knob to select how many silhouettes to view, and improved visualization of structure.

No precomputation is required to use silhouette edges during visualization. This ability to provide immediate response to the user makes the use of this technique attractive. It also provides the user the ability to try out the visualization and determine if they like it. Since there is no cost to experiment with it, they are more likely to use it on a regular basis. There is also only a single knob to adjust to control the level of silhouettes. Increasing the value will increase the number

of silhouettes, decreasing the value produces the opposite effect. The results of changing the parameters are also visible while the user is changing them, making the experience more explorative.

The utility of this method was readily apparent to the domain scientists shown. One, in fact, began to make immediate use of it even when I was not around. In reference to the Foam data set (see Figure 5.1), he indicated how impressed he was how well the structure became visible once silhouettes were used. This is a testimony of the attractiveness of this technique.

There is work to be done to improve this method. Currently the edges of the silhouettes can be jagged. A particle not represented by more than a handful of pixels can appear much larger and blocky. Silhouettes on these are useful, as particles that ordinarily would be missed now have some emphasis highlighting their whereabouts. A method to smooth out these edges, however, would better represent the shape of the object the silhouette is accentuating.

Another direction for future work would be to add gray levels to the silhouettes to indicate silhouettes of varying discontinuity. Thickness could also be used to accentuate greater differences in depth.

One final direction of future work would be to look at how to appropriately apply silhouette edges to multi sampled renderings. Saito and Takahashi average the depth for a given pixel and use that value when computing edges. This, however, will still produce jagged silhouettes. Perhaps the depth buffer could be stored with a higher resolution. Silhouettes would be computed with the depth buffer and applied with a width corresponding to a pixel size with gray levels darkest at the center and lightens at the edges.

### 5.3 Final comments

Silhouette edges are appropriate for particle visualization. They help aid in the perception of spatial relationships between particles, is easy to use, and can be used without precomputation time. Ambient occlusion textures make use of the human perception system by using an illumination technique that utilizes global position

information. There is also no need to have a user make choices about lighting conditions that could spoil the rendering. While there is little impact on rendering performance the precomputation time and memory requirements can inhibit the use of this method. This method is also only suited to static data that will not be cropped during rendering.

## REFERENCES

- [1] A. Glassner. *Principles of Digital Image Synthesis*. Morgan Kaufmann Publishers, San Francisco, California, 1995.
- [2] B. Gooch, P.-P. J. Sloan, A. Gooch, P. Shirley, and R. Riesenfeld. Interactive technical illustration. In *ACM Interactive 3D*, April 1999.
- [3] G. Greger, P. Shirley, P. Hubbard, and D. Greenberg. The irradiance volume. *IEEE Computer Graphics and Applications*, 18(2):32–43, 1998.
- [4] J. Guilkey and J. Weiss. An implicit time integration strategy for use with the material point method. In *Proceedings from the First MIT Conference on Computational Fluid and Solid Mechanics*, June 2001.
- [5] J. T. Kajiya. The rendering equation. In *Computer Graphics (Proceedings of SIGGRAPH)*, volume 20(4), pages 143–150, August 1986.
- [6] G. Kindlmann, R. Whitaker, T. Tasdizen, and T. Möller. Curvature-based transfer functions for direct volume rendering: Methods and applications. In *IEEE Visualization*, October 2003.
- [7] H. Landis. Production-ready global illumination. *Course 16 notes, SIGGRAPH 2002*, 2002. Available at <http://www.renderman.org/RMR/Books/sig02.course16.pdf.gz>.
- [8] M. D. McCool. Shadow volume reconstruction from depth maps. In *ACM Transactions on Graphics*, volume 19(1), pages 1–26, January 2001.
- [9] S. E. Palmer. *Vision Science*. The MIT Press, Cambridge, Massachusetts, 1999.
- [10] S. Parker, W. Martin, P.-P. J. Sloan, P. Shirley, B. Smits, and C. Hansen. Interactive ray tracing. In *Symposium on Interactive 3D Graphics*, pages 119–126, 1999.
- [11] T. Saito and T. Takahashi. Comprehensible rendering of 3-d shapes. In *Computer Graphics (Proceedings of SIGGRAPH)*, volume 24(4), pages 197–206, August 1990.
- [12] A. J. Stewart. Vicinity shading for enhanced perception of volumetric data. In *IEEE Visualization*, October 2003.

- [13] G. Ward, F. Rubinstein, and R. Clear. A ray tracing solution for diffuse interreflection. In *Proceedings of SIGGRAPH 1988*, Computer Graphics Proceedings, Annual Conference Series, pages 85–92. ACM, ACM Press / ACM SIGGRAPH, 1988.
- [14] C. Wyman, S. Parker, P. Shirley, and C. Hansen. Interactive display of isosurfaces with global illumination. In *TVCG*, ?????? 2004. Submitted for publication.